FEBS Letters 527 (2002) 86–90 FEBS 26415

The temperature dependence of the hydrogen exchange in the SH3 domain of α-spectrin

M. Sadqi, S. Casares, O. López-Mayorga, F. Conejero-Lara*

Departamento de Química Física e Instituto de Biotecnología, Facultad de Ciencias, Universidad de Granada, 18071 Granada, Spain

Received 13 June 2002; revised 16 July 2002; accepted 16 July 2002

First published online 12 August 2002

Edited by Thomas L. James

Abstract The amide hydrogen–deuterium exchange (HX) in the Src homology region 3 (SH3) domain of α-spectrin has been measured by nuclear magnetic resonance as a function of temperature between 8 and 46°C. The analysis of the temperature dependence of HX from a statistical thermodynamic point of view has allowed us to estimate the enthalpies and entropies of the conformational processes leading to HX. The results indicate that under native conditions the domain undergoes a wide variety of conformational fluctuations, ranging from local motions, mainly located in loops, turns and chain ends and involving only low enthalpy and entropy, to extensive structural disruptions affecting its core and involving enthalpies and entropies that come fairly close to those observed during global unfolding.

Key words: Amide hydrogen–deuterium exchange; Protein folding; Calorimetry; Src homology region 3 domain; Nuclear magnetic resonance

1. Introduction

One of the most promising techniques for exploring the protein folding landscape is that of amide hydrogen–deuterium exchange (HX) [1]. Nuclear magnetic resonance (NMR) measurements of HX allow us to characterize the conformational states of proteins, which might be infinitesimally populated under native conditions. In the 'native-state HX' method the rates of amide–HX are measured while the protein is progressively destabilized, usually with denaturants such as guanidinium chloride or urea. When HX occurs under EX2 conditions [2] the analysis of the data provides residue-specific free energies (ΔG_{ex}) and m values for the exchange-competent conformational states accessible from the native state, from which data we can derive conclusions about the structural nature of these forms. This technique has in favorable cases led to the characterization of partially folded intermediates [3–9]. Native-state HX has also been measured as a function of pressure [8,10], pH [11,12] and temperature [9,11,13–15]. Many of these analyses have relied upon simplified models, in which native-state HX is assumed to occur via either or both of two different, well-defined processes, i.e. a local fluctuation and/or a large partial or global unfolding [3,9,16]. On the other hand, experimental native HX patterns in proteins have been modelled reasonably well by considering them to be statistical ensembles of conformational states [17–20]. Very recently we described a statistical thermodynamic analysis of the pH dependence of the HX in the Src homology region 3 (SH3) domain of α-spectrin, in which we made no a priori assumptions about the number or nature of the conformational processes leading to the exchange [12]. The results were consistent with other studies, which support the view that HX occurs via a distribution of conformational states rather than discrete unfolding events [21–23]. We report here upon the temperature dependence of the HX in the SH3 domain of α-spectrin. An analysis of the data from a statistical thermodynamic point of view provides information about the thermodynamic properties of the conformational ensemble of states accessible to the domain under native conditions.

2. Materials and methods

The SH3 domain of wild-type chicken α-spectrin was isolated as described elsewhere [20]. Protein aliquots were extensively dialyzed against pure water and lyophilized. NMR-detected hydrogen–deuterium exchange experiments were performed at pH* (pH-meter reading for deuterium-oxide solutions uncorrected for isotopic effects) 3.0 and nine different temperatures between 8.3 and 45.8°C, as described elsewhere [20]. The exchange was initiated by rapidly dissolving the lyophilized protein in deuterated buffer (20 mM d_5-glycine at pH* 3.0). Samples were rapidly filtrated and put into the magnet's probe. The final protein concentration was about 4.5 mM. To determine accurately the temperature of the samples inside the NMR probe a temperature calibration curve was previously constructed using a PT-100 temperature sensor immersed in an NMR tube filled with 0.5 ml of silicone oil placed inside the magnet's probe. A set of 20–30 two-dimensional, phase-sensitive COSY spectra was acquired with a Brüker AMX-500 spectrometer during the time of exchange, as described elsewhere [20]. NMR spectra were processed and analyzed using NMRpipe [24] and NMRview [25]. The COSY NH-C_αH cross peaks were reassigned for each temperature taking as reference the published assignment at pH 3.5 and 35°C [26]. The decay in intensity of each NH-C_αH cross peak as a function of the exchange time was fitted to a single exponential decay function to determine the exchange-rate constants, k_{ex}, as described elsewhere [20]. Intrinsic exchange-rate constants for each amide proton, k_{int}, at pH* 3.0 were calculated using the exchange data for model peptides and taking into account the temperature dependences of the acid-, base- and water-catalyzed exchange-rate constants [27]. An EX2 mechanism for the amide–hydrogen exchange was assumed to be valid at pH* 3.0 throughout the whole experimental temperature range. The equilibrium constant, K_{op}, for the opening process rendering the amide hydrogen of any particular residue exchange-competent, was calculated as

*Corresponding author. Fax: (34)-958-272879.
E-mail address: conejero@ugr.es (F. Conejero-Lara).

Abbreviations: SH3, Src homology region 3; HX, amide hydrogen–deuterium exchange; pH*, pH-meter reading for deuterium-oxide solutions uncorrected for isotopic effects

0014-5793/02/$22.00
PII: S0014-5793(02)03172-1

$K_{op} = k_{ex}/k_{int}$. The apparent Gibbs energy difference between the open and closed states, referred to in this work as 'Gibbs energy of exchange', was obtained by

$$\Delta G_{ex} = -RT \ln K_{op} \quad (1)$$

3. Results and discussion

Amide–hydrogen exchange (HX) rates in the SH3 domain have been measured at pH* 3.0 by two-dimensional NMR at different temperatures between 8.3 and 45.8°C. At 45.8°C it was only possible to follow the HX rates of seven residues, whereas at 8.3 and 12.7°C we could measure the rates of 45 residues out of a possible 59. Residue-specific Gibbs energies of exchange, ΔG_{ex}, were calculated using Eq. 1. Fig. 1A shows the temperature dependence of ΔG_{ex} for several representative residues, in comparison with the temperature dependence of the Gibbs energy increment upon global unfolding of the domain, ΔG_{unf}, which we have measured previously by differential scanning calorimetry (DSC) in D_2O solutions under identical conditions [20]. At low temperatures the ΔG_{ex} values are quite disperse, ranging from 4.7 kJ mol^{-1} to 13.5 kJ mol^{-1}, which indicates a great variety of conformational processes leading to HX in this small domain. The ΔG_{ex} values for a majority of residues are significantly lower than ΔG_{unf} throughout the whole range of temperatures assayed, except for a few residues at temperatures below 25°C. For example, at 12.7°C only 11 residues have ΔG_{ex} values within the uncertainty band of ΔG_{unf}. The most protected residues in this low-temperature range are A11, W42 and K43. At 27.1°C, however, just W42 has a ΔG_{ex} value within the error band of ΔG_{unf} and only the ΔG_{ex} values of seven residues more fall at less than 1 kJ mol^{-1} out of this band. As temperature increases and the domain becomes less stable the ΔG_{ex} values become less disperse, indicating that fewer conformational processes are governing the exchange [9]. Nevertheless, it is surprising that as the global unfolding temperature is approached the ΔG_{ex} values do not in general converge with the ΔG_{unf} curve (see below).

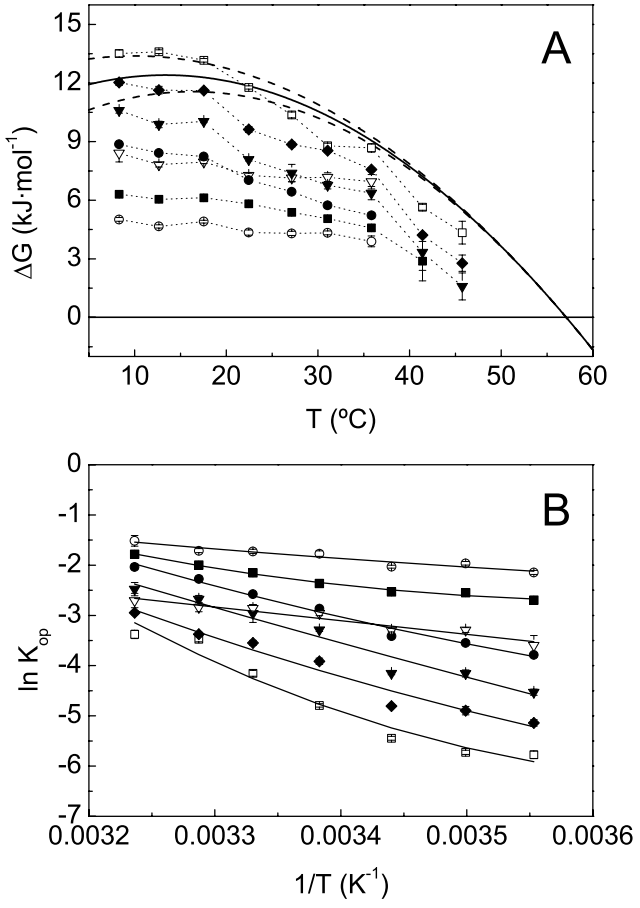

Fig. 1. A: The temperature dependence of the apparent Gibbs energy of HX, ΔG_{ex}, at pH* 3.0 for the following residues in SH3: L8 (■); V9 (▼); V23 (●); W42 (□); A56 (▽); V58 (◆); L61 (○). Error bars indicate the uncertainty in the ΔG_{ex} values estimated as described elsewhere [12]. Dotted lines connect the symbols for the sake of clarity. The solid line represents the temperature dependence of the change in Gibbs energy for the global unfolding of the domain, ΔG_{unf}, under identical conditions to those determined by DSC [20]. Dashed lines indicate the estimated uncertainty bands in ΔG_{unf}. B: Plots of the logarithm of the opening equilibrium constant, ln K_{op}, versus the inverse of temperature for the same residues in A. The solid lines represent the best fittings of the data between 8.3 and 35.8°C using Eq. 6.

We have interpreted the temperature dependence of native-state HX from a statistical thermodynamic point of view in a similar way to our previous analysis of the pH dependence of HX [12]. The opening equilibrium constant, K_{op}, for the amide hydrogen of a particular residue j can be defined in terms of probabilities of conformational states, P_i [17–20]:

$$K_{op,j} = \frac{\sum_{i(j,ex)} P_i}{\sum_{i(j,nex)} P_i} = \frac{\sum_{i(j,ex)} \exp\left(-\frac{\Delta G_i}{RT}\right)}{\sum_{i(j,nex)} \exp\left(-\frac{\Delta G_i}{RT}\right)} \quad (2)$$

where ΔG_i represents the Gibbs energy of each state compared to the native state. The sums (j,ex) and (j,nex) are applicable to all the exchange-competent and non-exchange-competent states respectively for the amide group of residue j.

The derivative of the logarithm of K_{op} versus temperature for residue j is

$$\frac{d\ln K_{op,j}}{dT} = \frac{\sum_{i(j,ex)} \frac{d}{dT}\left[\exp\left(-\frac{\Delta G_i}{RT}\right)\right]}{\sum_{i(j,ex)} \exp\left(-\frac{\Delta G_i}{RT}\right)} - \frac{\sum_{i(j,nex)} \frac{d}{dT}\left[\exp\left(-\frac{\Delta G_i}{RT}\right)\right]}{\sum_{i(j,nex)} \exp\left(-\frac{\Delta G_i}{RT}\right)}$$

$$= \frac{\sum_{i(j,ex)} \left[\exp\left(-\frac{\Delta G_i}{RT}\right)\right] \cdot \frac{\Delta H_i}{RT^2}}{\sum_{i(j,ex)} \exp\left(-\frac{\Delta G_i}{RT}\right)} - \frac{\sum_{i(j,nex)} \left[\exp\left(-\frac{\Delta G_i}{RT}\right)\right] \cdot \frac{\Delta H_i}{RT^2}}{\sum_{i(j,nex)} \exp\left(-\frac{\Delta G_i}{RT}\right)} \quad (3)$$

and dividing the numerator and denominator by the system partition function it holds that

$$\frac{d\ln K_{op,j}}{dT} = \frac{1}{RT^2}\left[\frac{\sum_{i(j,ex)} \Delta H_i P_i}{\sum_{i(j,ex)} P_i} - \frac{\sum_{i(j,nex)} \Delta H_i P_i}{\sum_{i(j,nex)} P_i}\right]$$

$$= \frac{\langle \Delta H \rangle_{(j,ex)} - \langle \Delta H \rangle_{(j,nex)}}{RT^2} = \frac{\Delta H_{ex,j}}{RT^2} \quad (4)$$

In this equation ΔH_i is the enthalpy of the state i relative to the native state. The quantity $\langle \Delta H \rangle_{(j,\mathrm{ex})}$ is the average enthalpy of all exchange-competent conformational states for residue j, whilst $\langle \Delta H \rangle_{(j,\mathrm{nex})}$ is the average enthalpy of all non-exchange-competent states (including the native state) for the same residue. Therefore, $\Delta H_{\mathrm{ex},j}$ represents the average net enthalpy change for the conformational fluctuations leading to exchange for residue j.

Using the relationship $\mathrm{d}y/\mathrm{d}(1/x) = -x^2 \cdot \mathrm{d}y/\mathrm{d}x$, Eq. 4 can be rewritten as

$$\frac{\mathrm{d}\ln K_{\mathrm{op},j}}{\mathrm{d}(1/T)} = -\frac{\Delta H_{\mathrm{ex},j}}{R} \tag{5}$$

Eq. 5 allows us to determine the average net enthalpy, ΔH_{ex}, of the conformational changes responsible for the exchange of each residue from the slope of a plot of $\ln K_{\mathrm{op}}$ versus $1/T$. Accordingly, the temperature dependence of HX provides residue-specific thermodynamic information about the ensemble of conformations of proteins under native conditions.

Fig. 1B represents $\ln K_{\mathrm{op}}$ versus $1/T$ for the same set of residues as Fig. 1A. It is evident in the figure that the plot for some residues is appreciably curved, which means that ΔH_{ex} depends upon temperature for these residues. For other residues, however, the plot of $\ln K_{\mathrm{op}}$ versus $1/T$ is more linear. Using Eq. 4 it can be easily demonstrated that the derivative of $\Delta H_{\mathrm{ex},j}$ versus temperature has the typical statistical meaning of an increase in heat capacity, $\Delta C_{p(\mathrm{ex},j)}$, associated with the conformational processes leading to the HX of residue j (not shown). This quantity can be related to the average net exposure of surface to the solvent associated to the exchange of the residue. Assuming $\Delta C_{p(\mathrm{ex},j)}$ to be more or less independent of temperature, the integrated form of Eq. 5 is

$$\ln K_{\mathrm{op},j} = \ln K^0_{\mathrm{op},j} - \frac{(\Delta H^0_{\mathrm{ex},j} - \Delta C_{p(\mathrm{ex},j)} \cdot T_0)}{R}\left(\frac{1}{T} - \frac{1}{T_0}\right) + \frac{\Delta C_{p(\mathrm{ex},j)}}{R}\ln\left(\frac{T}{T_0}\right) \tag{6}$$

where T_0 is a reference temperature and $\ln K^0_{\mathrm{op},j}$ and $\Delta H^0_{\mathrm{ex},j}$ are the respective magnitudes for residue j at $T = T_0$. Using Eq. 6, the data of $\ln K_{\mathrm{op}}$ versus $1/T$ could be fitted to obtain both ΔH_{ex} and $\Delta C_{p(\mathrm{ex})}$ for each residue. Unfortunately, the $\Delta C_{p(\mathrm{ex})}$ values cannot be accurately determined due to the scattering of experimental data. Therefore, we have used $\Delta C_{p(\mathrm{ex})}$ in each fitting merely as an operational parameter to determine ΔH_{ex} at 25°C for each residue using Eq. 6. These fittings (Fig. 1B) were made using the $\ln K_{\mathrm{op}}$ data in the temperature range between 8.3 and 35.8°C, in which the HX of the majority of the residues could be measured.

Similarly to the previous analysis, the temperature derivative of ΔG_{ex} for residue j can also be calculated easily using Eqs. 1 and 2, thus

$$\frac{\mathrm{d}\Delta G_{\mathrm{ex},j}}{\mathrm{d}T} = -\frac{\Delta H_{\mathrm{ex},j}}{T} + \frac{\Delta G_{\mathrm{ex},j}}{T} = -\Delta S_{\mathrm{ex},j} \tag{7}$$

In this equation $\Delta S_{\mathrm{ex},j}$ represents the apparent entropy change accompanying the HX process for residue j and can be calculated either from the slope of the plots of $\Delta G_{\mathrm{ex},j}$ versus T or from the values of $\Delta G_{\mathrm{ex},j}$ and $\Delta H_{\mathrm{ex},j}$ using Eq. 7.

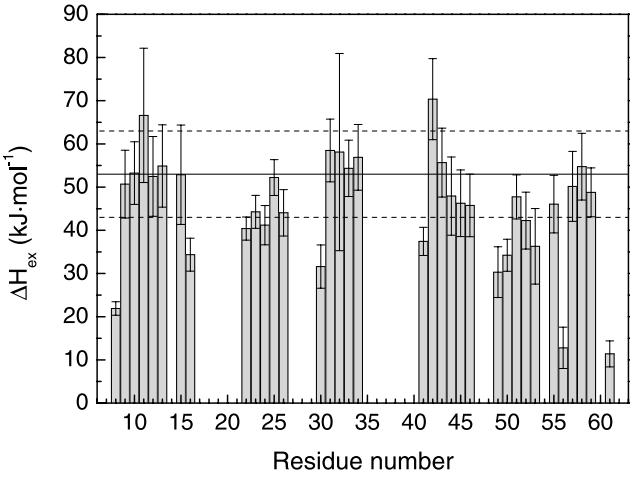

Fig. 2. The average net enthalpy of HX, ΔH_{ex}, for each residue in SH3 at pH* 3.0 and 25°C. Values of ΔH_{ex} are represented in columns. Error bars at the top of each column represent the standard errors of the ΔH_{ex} values estimated from the fittings using Eq. 6. The solid horizontal line indicates the change in the enthalpy of global unfolding, ΔH_{unf}, under the same conditions. Dashed lines indicate the uncertainty in ΔH_{unf}.

The results of the analysis described here are plotted in Fig. 2. The ΔH_{ex} values at 25°C range between 11 and 70 kJ mol^{-1}, which is consistent with a broad diversity of conformational changes leading to the exchange in the SH3 domain [12,20]. The enthalpy change of global unfolding, ΔH_{unf}, measured by DSC at different pH* values in D_2O buffer has been reported elsewhere [20]. Extrapolation of the DSC data using the reported change in the heat capacity of unfolding gives an estimate for ΔH_{unf} of 53 ± 10 kJ mol^{-1} at 25°C. Two partially compensating effects have been proposed to be mainly responsible for the enthalpy change in protein unfolding: the disruption of internal interactions within the protein molecule (van der Waals, hydrogen bonds, electrostatic interactions, etc.) and the hydration of buried protein groups, which become exposed upon unfolding [28,29]. There is a relatively large set of residues in the central part of the β-sheets and the 3_{10} helix belonging to the domain's core, with ΔH_{ex} values similar to ΔH_{unf}, which implies a net balance of interactions for the conformational changes leading to HX comparable to that of global unfolding. Some residues located near to or within the loops, turns or chain ends have lower ΔH_{ex} values, suggesting that HX occurs via more localized fluctuations involving a lower number of contacts. We could not determine the ΔH_{ex} values for a number of residues, either because their HX could not be followed through a wide enough temperature range or because it could not be measured at all. Most of these residues are also situated in or near the loops, turns or chain ends.

The ΔS_{ex} values at 25°C have a pattern very similar to those of ΔH_{ex} (results not shown). Once more, for most residues in the domain's core ΔS_{ex} is similar to or higher than ΔS_{unf}. Entropy changes upon protein unfolding are also the result of the balance between an increase in the conformational disorder of the polypeptide chain and a reduction in the degree of freedom of water molecules upon the solvation of buried protein surfaces [30]. These results are also consistent with the need for a considerable structural disordering of the core regions to take place for HX to occur. Other residues show

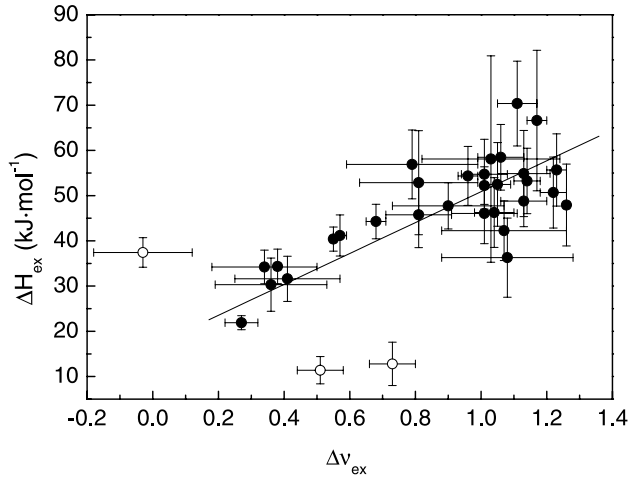

Fig. 3. Plots of ΔH_{ex} versus $\Delta\nu_{ex}$ for the HX of SH3 at pH* 3.0 and 25°C. Symbols represent the data for each residue. Error bars indicate the uncertainties of both magnitudes. The line indicates the linear correlation obtained for these two magnitudes ($r = 0.90$) excluding the data of W41, A56 and L61, which are represented by open symbols.

lower ΔS_{ex} values, in agreement with their HX occurring via more localized fluctuations.

According to these results the SH3 domain undergoes a wide variety of conformational fluctuations under native conditions, which range from local motions of low enthalpy and entropy to extensive structural disruptions with enthalpies and entropies approaching those observed for global unfolding. The relatively large errors associated with the determination of both ΔH_{ex} and ΔS_{ex} do not allow us, however, to draw conclusions about the thermodynamic reasons for the discrepancy between ΔG_{ex} and ΔG_{unf} found for most of the residues. Additionally, we found a strong compensation between ΔH_{ex} and ΔS_{ex} for all the residues (not shown) as has also been reported elsewhere [8].

We have recently reported the effect of pH on the values of ΔG_{ex} for the SH3 domain [12]. From an analysis of the data we obtained the average uptake of protons, $\Delta\nu_{ex}$, coupled with the HX of each residue. These data provided residue-specific information about the extent to which the electrostatic interactions in the domain are affected by the conformational changes leading to HX, and gave an estimation of the structural disruption associated with native fluctuations for this domain. Fig. 3 represents ΔH_{ex} versus $\Delta\nu_{ex}$ for those residues of SH3 for which both quantities could be calculated. Both magnitudes appear to be correlated ($r = 0.90$) except for three residues (W41, A56 and L61). A very similar correlation occurs between ΔS_{ex} and $\Delta\nu_{ex}$ (not shown). These results support the view that the native SH3 domain is an ensemble of conformational states characterized by a broad range of enthalpy and entropy values, which correlate well with the degree of disruption of their electrostatic interactions and, therefore, their structural disorder. These correlations illustrate the potential of this type of analysis of native-state HX measurements to explore both the thermodynamic and structural properties of the protein folding landscape.

Finally, it has been reported elsewhere that the SH3 domain of α-spectrin folds and refolds in a single two-state transition, without the presence of stable intermediates [31–33]. Thus it might be expected that as the unfolding temperature, T_m (where $\Delta G_{unf} = 0$), is being approached, global unfolding would dominate the hydrogen exchange and consequently the ΔG_{ex} values for all the residues would converge with the ΔG_{unf} curve. As can be seen in Fig. 1A, however, this in general does not occur. For many residues the ΔG_{ex} dependence shows a tendency to pass through $\Delta G = 0$ at temperatures significantly lower than the unfolding T_m. Among the residues for which ΔG_{ex} values are measurable above 40°C, this is particularly evident for L8, V9, or V58, in addition to other residues not shown in the figure. Another group of residues (W42 for instance, in Fig. 1) show ΔG_{ex} dependences versus temperature closer to the ΔG_{unf} curve. These observations suggest that as the global unfolding transition is being approached a conformational state or states other than the globally unfolded state might well turn out to be important in the HX of this domain. The ΔG_{ex} values above 40°C for some of the residues are below 5 kJ mol^{-1}, indicating that these states become significantly populated at these temperatures. This would be at odds with the absence of detectable folding intermediates for the SH3 domain of α-spectrin [31–33]. It has been shown recently that well-populated folding intermediates detectable by HX measurements may elude the standard analysis of unfolding data [34]. Our results encourage us in the search for new evidence to confirm the existence of stable intermediate states of the SH3 domain under certain conditions.

Acknowledgements: We thank the CIC of the University of Granada for their technical support in the NMR experiments. We also thank Dr. J. Trout for revising the English text. This work was financed by grants PL96-2180 from the European Union and PB96-1446 and BIO2000-1459 from the Spanish Ministry of Science and Technology.

References

[1] Englander, S.W. (2000) Annu. Rev. Biophys. Biomol. Struct. 29, 213–238.
[2] Hvidt, A. and Nielsen, S.O. (1966) Adv. Protein Chem. 21, 287–386.
[3] Bai, Y., Sosnick, T.R., Mayne, L. and Englander, S.W. (1995) Science 269, 192–197.
[4] Chamberlain, A.K., Handel, T.M. and Marqusee, S. (1996) Nat. Struct. Biol. 3, 782–787.
[5] Bai, Y. and Englander, S.W. (1996) Proteins 24, 145–151.
[6] Hiller, R., Zhou, Z.H., Adams, M.W.W. and Englander, S.W. (1997) Proc. Natl. Acad. Sci. USA 94, 11329–11332.
[7] Englander, S.W., Mayne, L.C., Bai, Y. and Sosnick, T.R. (1997) Protein Sci. 6, 1101–1109.
[8] Fuentes, E.J. and Wand, A.J. (1998) Biochemistry 37, 3687–3698.
[9] Milne, J.S., Xu, Y., Mayne, L.C. and Englander, S.W. (1999) J. Mol. Biol. 290, 811–822.
[10] Hitchens, T.K. and Bryant, R.G. (1998) Biochemistry 37, 5878–5887.
[11] Swint-Kurse, L. and Roberston, A.D. (1996) Biochemistry 35, 171–180.
[12] Sadqi, M., Casares, S., López-Mayorga, O., Martínez, J.C. and Conejero-Lara, F. (2002) FEBS Lett. 514, 295–299.
[13] Thomsen, N.K. and Poulsen, F.M. (1993) J. Mol. Biol. 234, 234–241.
[14] Itzhaki, L.S., Neira, J.L. and Fersht, A.R. (1997) J. Mol. Biol. 270, 89–98.
[15] Neira, J.L. and Mateu, M.G. (2001) Eur. J. Biochem. 268, 4868–4877.
[16] Woodward, C., Simon, I. and Tüchsen, E. (1982) Mol. Cell. Biochem. 48, 135–160.
[17] Hilser, J.V. and Freire, E. (1996) J. Mol. Biol. 262, 756–772.
[18] Hilser, J.V. and Freire, E. (1997) Proteins 27, 171–183.
[19] Hilser, J.V., Dowdy, D., Oas, T.G. and Freire, E. (1998) Proc. Natl. Acad. Sci. USA 95, 9903–9908.

[20] Sadqi, M., Casares, S., Abril, M.A., López-Mayorga, O., Conejero-Lara, F. and Freire, E. (1999) Biochemistry 38, 8899–8906.
[21] Arrington, C.B., Teesch, L.M. and Robertson, A.D. (1999) J. Mol. Biol. 285, 1265–1275.
[22] Arrington, C.B. and Robertson, A.D. (2000) J. Mol. Biol. 300, 221–232.
[23] Parker, M.J. and Marqusee, S. (2000) J. Mol. Biol. 300, 1361–1375.
[24] Delaglio, F., Grzesiek, S., Vuister, G.W., Zhu, G., Pfeifer, J. and Bax, A. (1995) J. Biomol. NMR 6, 277–293.
[25] Johnson, B.A. and Blevins, R.A. (1994) J. Biomol. NMR 4, 603–614.
[26] Blanco, F.J., Ortiz, A.R. and Serrano, L. (1997) J. Biomol. NMR 9, 347–357.
[27] Bai, Y., Milne, J.S., Mayne, L. and Englander, S.W. (1993) Proteins 17, 75–86.
[28] Makhatadze, G.I. and Privalov, P.L. (1993) J. Mol. Biol. 232, 639–659.
[29] Hilser, V.J., Gómez, J. and Freire, E. (1996) Proteins 26, 123–133.
[30] Makhatadze, G.I. and Privalov, P.L. (1996) Protein Sci. 5, 507–510.
[31] Viguera, A.R., Martinez, J.C., Filimonov, V.V., Mateo, P.L. and Serrano, L. (1994) Biochemistry 33, 2142–2150.
[32] Martínez, J.C., Pisabarro, M.T. and Serrano, L. (1998) Nat. Struct. Biol. 5, 721–729.
[33] Martínez, J.C. and Serrano, L. (1999) Nat. Struct. Biol. 6, 1010–1016.
[34] Mayne, L. and Englander, S.W. (2000) Protein Sci. 9, 1873–1877.